DEVELOPMENTS IN MESOSCALE MODELING AND SATELLITE SAR IMAGING OF OFFSHORE WIND MAPS

B. H. Jørgensen[+], B. Furevik[*], C. B. Hasager[+], P. Astrup[+], O. Rathmann[+], R. Barthelmie[+], S. Pryor[+]

[+]Risø National Laboratory, Wind Energy Department,
DK-4000 Roskilde, Denmark, Phone +45 4677 5471 / Fax +45 4677 5970; bo.hoffmann@risoe.dk

[*]Nansen Environmental and Remote Sensing Center
Edvard Griegsvei 3A, N-5059 Bergen, Norway. Phone +47 55297288, Fax +47 5520 0050

ABSTRACT: New developments for obtaining offshore wind maps by meso-scale modeling and satellite Synthetic Aperture Radar (SAR) images are presented. Results for Maddalena in Italy are compared to earlier results from Horns Rev in Denmark. The wind field in coastal regions is simulated with the Karlsruhe Atmospheric Mesoscale Model 2 (KAMM2). Data (4 times daily) from the global reanalysis of NCEP/NCAR is used to obtain the geostrophic wind and other large scale forcings which are suitable as input to the mesoscale model. This approach has mainly been used for regions on land. In coastal areas the wind fields can be complicated due to stability effects and the influence of land topography for offshore wind directions. The results of the simulations are compared with wind speeds and directions derived from satellite SAR images. In addition, results from WAsP of Risø National Laboratory are incorporated. The current empirical algorithms used for obtaining the wind speed from the radar backscatter arecalibrated for the open sea. Therefore, the mesoscale model and WAsP are also useful for comparison with the SAR-derived wind speeds close to the shore.
Keywords: Offshore, wind, boundary layer, mesoscale model

1 INTRODUCTION

1.1 Background

Prediction of wind resources normally requires at least one year of wind observations from meteorological masts. For offshore sites, the masts are usually positioned in the sea or at the coastline. Sources of long term measured meteorological data are often not available. Therefore, mesoscale modeling using large scale forcing derived from reanalysis data [6] is used for obtaining the wind field. Offshore meteorological measurements are generally costly to perform. Thus, it seems natural to also utilize mesoscale modeling for offshore locations. However, the experience for the prediction of offshore wind resources with mesoscale modeling is rather limited. Wind speed maps based on satellite Synthetic Aperture Radar (SAR) images provide useful information relevant for offshore wind resource estimation at a relatively low cost. But, little experience exists for the estimation of offshore wind resources with satellite SAR images.

A previos study [8] using both mesoscale modeling and satellite SAR images has been performed for the Horns Rev offshore site in Denmark where ELSAM/ELTRA is planning a large wind farm [1]. In the present work, results are presented for the Maddalena offshore site in Italy, located in the Mezzo Passo strait between Sardinia and Corsica. Wind speeds and wind directions determined from the satellite images are investigated.

We have performed calculations with the non-hydrostatic Karlsruhe Atmospheric Mesoscale Model 2 (KAMM2) in order to validate the SAR derived wind speed maps near the coast line. In addition, we are using the SAR images to evaluate the performance of the mesoscale model far from the coast line.

Satellite images from Synthetic Aperture Radar (SAR) can be processed to provide maps of ocean wind speed. The data are of a high spatial resolution sampled three times a month. Radar looks through clouds and rain, so it works in all weather conditions.

Data used in the current work consists of 9 cases originating from the ERS SAR system providing images of backscatter coefficients that are used to calculate wind speed and direction in a 100 km * 100 km area.

It is expected that large ensembles of SAR images can be used to estimate off-shore wind climates. The main disadvantage is the low temporal coverage, however, comparison [13] with measurement data indicate that relatively few scenes (50-100) selected randomly from once per day satellite images should give the mean wind speed with a mean absolute error of less than 10% (disregarding algorithm error and provided that the diurnal cycle of wind speeds is small or well-represented by the sampling).

2 THE MODELS

2.1 The mesoscale model KAMM2

The Karlsruhe Atmospheric Mesoscale Model 2 (KAMM2) is a three-dimensional, non-hydrostatic, and compressible meso-scale model [2] related to KAMM [3,4]. Spatial derivatives are calculated in the model by central differences on a terrain following grid. The turbulent fluxes are parameterized using a mixing-length model with stability dependent turbulent diffusion coefficients in stably stratified flow, and a non-local closure for the convective mixed layer. Lateral boundary conditions assume zero gradients normal to the inflow sides. On outflow boundaries, the horizontal equations of motion are replaced by a simple wave equation allowing signals to pass out of the domain without reflection. Gravity waves are absorbed in the upper part of the computational domain which acts as a damping layer.

The model has been extended with a fetch-dependent sea roughness [5]. At initialization, the orography (see Figure 1), roughness, and large scale forcing (see 2.2) is loaded into the model.

The present calculations have been performed with a grid containing 101*101*61 cells for an area of 150 km*150 km, i.e. 1.5 km horizontal resolution. A run with 2 km resolution was performed to check grid independence and a run with 1 km resolution is underways.

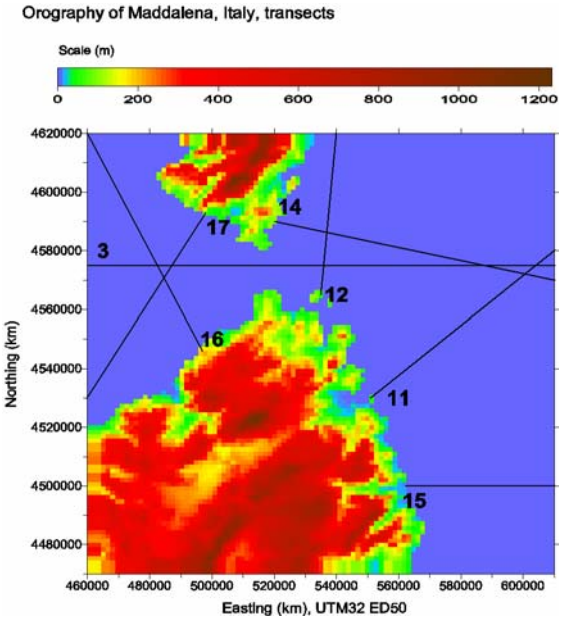

Figure 1. Orography near Maddalena, Italy, used in the mesoscale model. A number of transects proceeding from land towards the sea are depicted.

2.2 Large-scale forcing

Data (4 times daily) from the global reanalysis of NCEP/NCAR [6] is used to obtain the geostrophic wind and other large scale forcing (vertical air temperature gradient, air temperature at 2 m height, and temperature at land and sea) which is suitable as input to the meso-scale model. KAMM2 is able to run as a "stand-alone" model, i.e. the model can be run by using only the large scale forcing from the reanalysis (see sketch in Figure 2).

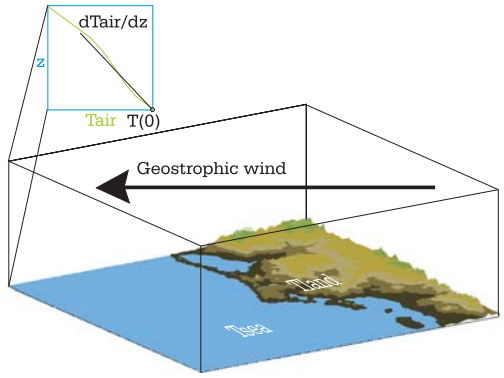

Figure 2. Sketch of the large scale forcing used for KAMM2 calculations.

Hence, it is not necessary to nest the meso-scale model within a larger model supplying the boundary conditions. For each case, the time of the reanalysis data is chosen as close as possible to the time of the satellite overpassing.

2.3 The micro scale WAsP model

WAsP [7] is a linear spectral wind flow model for slightly complex terrain. Based on the orography and roughness, it calculates the perturbations induced in a known background flow that is otherwise in equilibrium with a flat area with uniform roughness. The sum of the perturbations and background flow gives the final flow field.

The background flow in the current work is obtained from wind speed measurements of the Maddalena meteorological mast.

3 THE SATELLITE AND MAST DATA

3.1 Satellite SAR images

Satellite SAR data are available from the European ERS-2 and the Canadian RADARSAT-1. These SAR sensors are C-band (wavelength around 5 cm).

ERS SAR data have a repeat track of about 10 days and a 100 km swath. Hence, the area of each scene is viewed approximately three times per month (at mid-latitudes). Each scene is 100 km * 100 km and the raw resolution of the cells is 30 m * 30 m.

The measured quantity in each resolution cell is the backscatter coefficient (the normalised radar cross section), which is dependent upon the relative wind direction (zero for a wind blowing against the radar), the local radar beam incidence angle of the target area and the wind speed. This is described in Hasager *et al.* [9].

The SAR wind speed retrieval method originates from C-band scatterometer model CMOD-IFR2 [10], which is based on correlation analysis between global ocean buoy data and C-band scatterometer data. The ERS SAR wind maps are produced using wind directions obtained from streaks in the radar backscatter images where possible and otherwise under the assumption that the wind directions are known from observations at 10 m height.

The model coefficients depend on the incidence angle and wind speed given by look-up tables [10]. The typical resulting accuracy, solving for wind direction, is ±20° and, solving for wind speed, 2 m s^{-1} or 10% (RMS) for wind speeds between 2-24 m s^{-1} [11]. The wind speed is derived for a nominal height of 10 m above sea level.

The physical principle of C-band SAR backscatter coefficients and wind speed is given through the aerodynamic roughness (surface stress). The SAR-derived wind speed is obtained from radar backscatter due to the water roughness generated by the interaction between the wind and capillary and short gravity waves. In fetch-limited seas additional parameters may influence the roughness of the sea as compared to that of the open sea, in particular due to wave age, water depth, tidal currents, and atmospheric stability. However, the current algorithms used for obtaining the wind speed from the backscatter are calibrated for open sea conditions.

3.2 Selection of SAR images to describe climatology

Satellite SAR data was selected to represent part of the relevant wind climatology for the Maddalena site. From May 1996 to December 1997, a series of 5 cases corresponding to different weather conditions were obtained from the European Space Agency and analyzed. The cases of the data set is listed in Table I. Also listed in

the table are the corresponding reanalysis data cases for the time slots (four times daily) closest to the satellite overpassings.

3.3 Offshore mast observations at Maddalena

At Maddalena, Italy, a 10 m tall meteorological mast positioned has been equipped with wind speed and wind direction sensors. These data have been analysed to yield the hourly mean wind speed at 10 m and wind direction for the selected cases listed in Table II. The selected cases contains wind speed data in three regimes: low (3 - 9 m/s) 3 cases, medium (9-13 m/s) 1 case and high (13-18 m/s) 1 case. The speed and direction for the surface wind at 10 m height of the corresponding cases of the reanalysis data are also listed in the table. The surface wind of the reanalysis data does not represent the actual wind at the location of the mast – rather it is a measure of the large scale wind for a reanalysis grid cell. But it does give an impression of how realistic it is to apply the large scale forcing to the mesoscale model for the single cases. In addition, listed in the table are wind directions extracted from the SAR scenes near the location of the mast. Only in the two selected cases 1 and 5 were the wind streaks in the images sufficiently clear for the wind directions to be found without problems. It is seen that the SAR derived wind directions near Maddalena are close to the in-situ data for these two cases.

Table I. Dates and times of ERS SAR scenes from Maddalena and corresponding reanalysis cases.

Case	SAR scene		Reanalysis	
	Date	Time (UTC)	Date	Time (UTC)
1	1997.05.21	21.37	1997.05.22	00.00
2	1997.12.27	10.06	1997.12.27	12.00
3	1998.04.11	10.06	1998.04.11	12.00
4	1998.07.25	10.06	1998.07.25	12.00
5	1998.12.12	10.06	1998.12.12	12.00

Table II. Comparison of in-situ and reanalysis wind speed and direction for Maddalena. Comparison with SAR wind direction. SAR values taken from the coordinates UTM32: E532782.9, N4562053.7.

Case	In-situ		Reanalysis		SAR
	Speed (m/s)	Dir (deg)	Speed (m/s)	Dir (deg)	Dir (deg)
1	8.8	237.7	10.82	287.0	240.3
2	15.5	285.1	11.19	312.0	282.0
3	7.5	212.6	10.20	232.0	139.3
4	11.2	255.9	4.44	255.0	247.0
5	7.9	18.7	9.58	18.0	337.3

3.4 Selection of SAR scenes to compare with models

In order to compare the SAR derived wind speed maps with the mesoscale model results, it is necessary to select a subset of the SAR scenes for which the wind speed measured at the mast is constant for at least a few hours and compares well with the surface wind speed at 10m height from the reanalysis data. This is because the mesoscale model cannot be expected to perform very well if the applied large scale forcing is not realistic or frontal activity appears. Figure 3 shows, for case 1, that the wind speed and direction measured at the mast is relatively close to the surface wind at 10m height from the reanalysis data and a large change in wind speed happened 2 hours prior to the satellite overpass. This may be caused by a front. Weather charts from DWD [12] were checked for fronts. As seen in Table II the differences between in-situ and reanalysis data varied from 2 to 7 m/s and between 1 to 50 degrees.

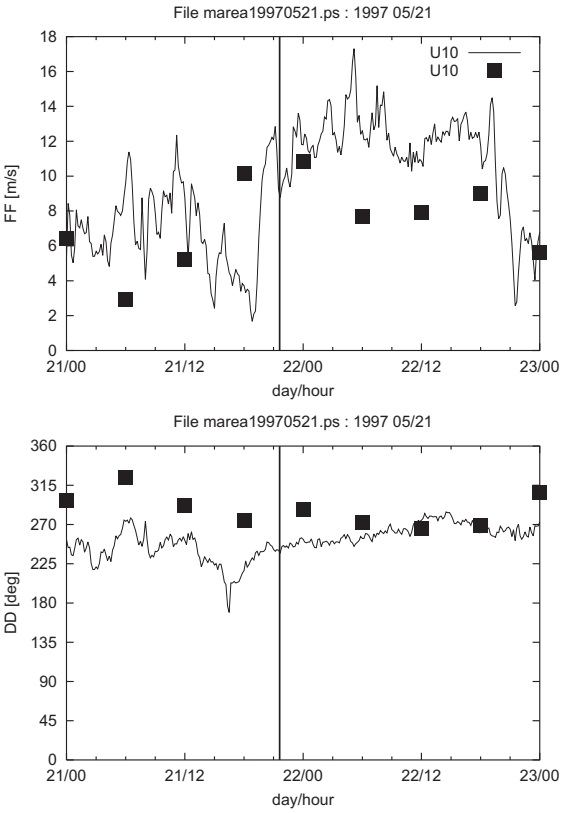

Figure 3. Wind speed (above) and wind direction (below) measured at the mast at Maddalena compared to the surface wind at 10m height from the reanalysis data (filled boxes). The satellite overpassing corresponding to case 1 is indicated with a vertical line.

4 RESULTS AND DISCUSSION

The mesoscale model results for case 1 are shown in Figure 4. The wind speed at 10 m (agl.) is depicted for 1.5 km horizontal resolution after 8 hours of simulation time. It is evident that the land topography has a significant influence on the offshore wind field. In general, the wind is westerly. Relatively high wind speeds are found in the strait in between Sardinia and Corsica. This feature is also found in the satellite SAR derived wind speeds shown in Figure 5. It must be noted that the SAR dervied wind speeds are only valid over water and not on land. From Table II the deviation in wind direction between in-situ data and reanalysis data is clear. This may explain why the wind direction results of the mesoscale model (which is using the reanalysis data) deviate significantly from the SAR derived wind direction whereas the SAR wind directions compares well to the in-situ data for case 1 and 2.

The satellite SAR derived wind speeds, the mesoscale model results and the WAsP results is plotted along the

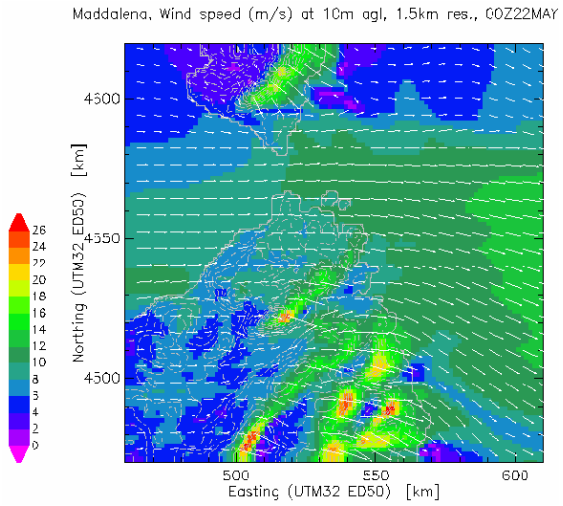

Figure 4. Mesoscale model results for case 1. The wind speed at 10 m height (agl.) is shown in the computational domain for 1.5 km horizontal resolution after 8 hours of simulation time.

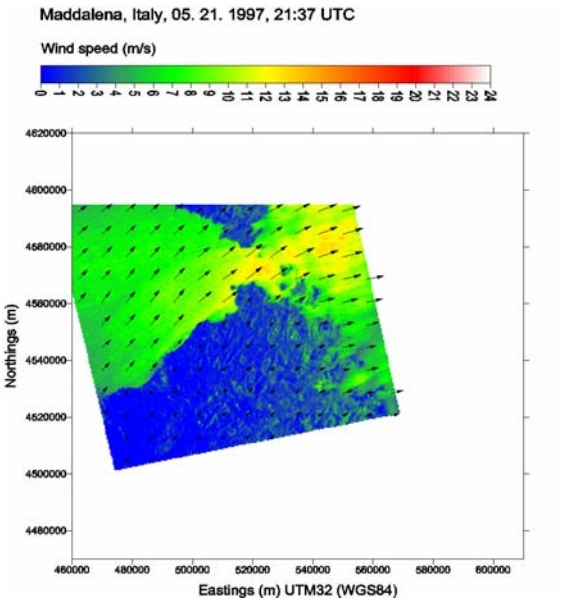

Figure 5. SAR derived wind speeds at 10 m height (agl.) for case 1.

horizontal transect 19 shown in the local orography map in Figure 6.

Figure 7 shows wind speeds for case 1. The transect position is shown at the x-axis. For this particular transect the wind field of the meso scale model does not model the roughness change from land to sea preceeding the start of the transect. The in-situ wind direction is from SW whereas the model wind direction is from WNW (Table II). On the contrary, WAsP clearly senses the land–sea roughness change because it is using the in-situ data as input. In accordance with the expected speed up of the wind offshore the SAR dervied wind speed is seen to increase along the first 4 km of the transect. Further out at sea, the general levels of the wind speed of SAR and the mesoscale model have a correspondence within the expected margin of error of 2 m/s. However, the SAR based wind speed maps capture features not present in the

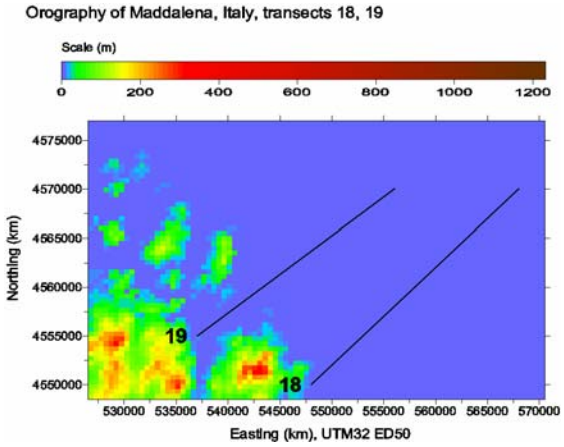

Figure 6. Local orography near Maddalena, Italy. The two transects labelled 18 and 19 proceeding from land towards the sea are depicted.

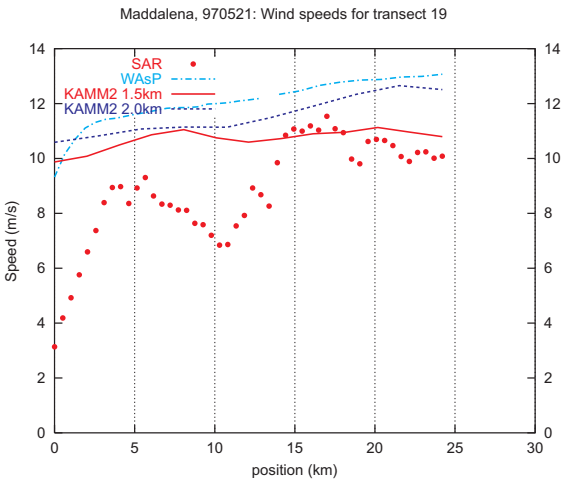

Figure 7. Wind speeds derived from SAR compared to the corresponding mesoscale model results for two different horizontal resolutions along the transect 19 shown in Figure 6. Also shown is the wind speed calculated with WAsP.

model results. In other investigated cases, a similar oscillating behavior of the SAR derived wind speeds with transect position is observed. These features may be caused by mechanisms similar to land-sea breezes driven by horizontal temperature gradients in the sea temperature or deviations in the SAR derived wind speeds due to physical phenomena related to the fetch limitations. In comparison to the earlier study [8] of Horns Rev, it is found that the general trend of the SAR based wind speed is followed closer to the shore by the mesoscale model results at the Maddalena site than at Horns Rev. This might be explained by differences in water depths at the two locations.

The comparison of wind directions for case 1 are shown in Figure 8. There is an offset between the wind direction of the mesoscale model results and the SAR data due to the fact that the model was run with a wind direction different from the in-situ observations.

The mesoscale model results are quite similar for the two different horizontal resolutions of 1.5 km and 2 km. We find in general that a resolution of 1.5 km is sufficient for mesoscale calculations at Maddalena.

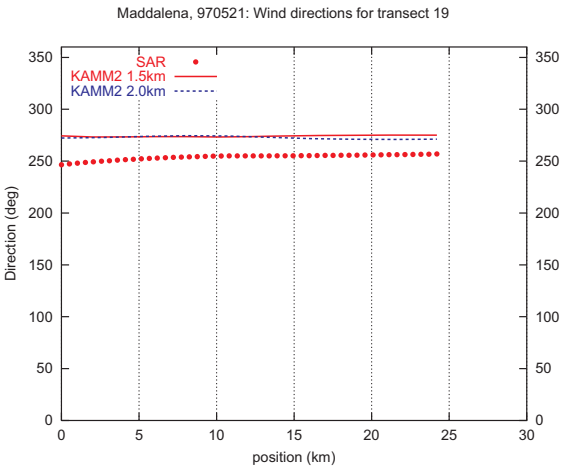

Figure 8. Wind directions derived from SAR streaks compared to the mesoscale model results calculated for two different horizontal resolutions along the transect 19 shown in Figure 6.

A further check for grid indepence is currently being performed at 1 km resolution. However, the solution is computationally intensive because of the current setup of the model. In addition to having a large number of grid cells (150x150x60) for 1 km resolution, it has also been found that the model is sensitive to non-smoothness of the grid near the surface. More filtering of the orography is required near the boundaries for complex terrain. At present, initial disturbances occur in the solution due to non-smoothness of the grid at high resolution. It requires long integration times for the model to transport the disturbances out of the computational domain as compared to the integration time necessary to complete the runs for coarser resolutions. A different filtering scheme for complex orography may considerably shorten the integration times.

5 CONCLUSION

A spatial comparison of satellite SAR derived wind speed maps to results from the mesoscale model KAMM2 and the linear spectral model WAsP has been performed for the offshore area near Maddalena, Italy. The mesoscale model largely follow general trends in the SAR based wind maps. Compared to the earlier study for Horns Rev, this behavior is found closer to the shore the Maddalena site. However, SAR based wind speed maps capture local features not present in the model results.

Analysis on wind streaks in the SAR scenes has been carried out. This has been tested against the wind directions measured at the mast and the mesoscale model results. Data from different geographical locations have been analyzed to ensure the applicability of ERS SAR wind speed maps for offshore wind resource assessment under different atmospheric and climatic conditions.

6 ACKNOWLEDGEMENTS

The present work was funded by the EU project WEMSAR (Wind Energy Mapping using Synthetic Aperture Radar) ERK6-CT-1999-00017. Satellite data are from ESA AO3-153.

REFERENCES

[1] S. Neckelmann, J. Petersen, Evaluation of the stand-alone wind and wave measurement systems for the Horns Rev 150 MW offshore wind farm in Denmark. Proceedings to OWEMES 2000, Offshore wind energy in Mediterranean and other European Seas, (2000) 17-27.

[2] G. Adrian, “Das Karlsruher Atmosphärische Mesoskalige Modell KAMM,” Prof. Dr. Franz Fiedler zum 60. Geburtstag, VBIMK, **21**, editor K. D. Beheng, IMK, 1998, Karlsruhe, Germany.

[3] G. Adrian and F. Fiedler, “Simulation of unstationary wind and temperature fields over complex terrain and comparison with observations,” Beitr. Phys. Atmos., **64**, (1991) 27-48.

[4] G. Adrian, “Zur Dynamik des Windfeldes über orographisch gegliedertem Gelände,” *Ber. Deutscher Wetterdienst*, **188**, (1994) 1-142.

[5] H. P. Frank, S. Larsen, and J. Højstrup, “Simulated Wind Power Off-shore Using Different Parametrizations for the Sea Surface Roughness,” *Wind Energ.*, **3**, 67-79 (2000).

[6] NCEP Reanalysis data provided by the NOAA-CIRES Climate Diagnostics Center, Boulder, Colorado, USA, from their Web site at http://www.cdc.noaa.gov/

[7] I. Troen and E. L. Petersen (1989). *European Wind Atlas*. ISBN 87-550-1482-8. Risø National Laboratory, Roskilde. 656 pp.

[8] B. H. Jørgensen, B. Furevik, C. B. Hasager, P. Astrup, O. Rathmann, R. Barthelmie, S. Pryor. “Off-shore wind fields obtained from mesoscale modeling and satellite SAR images,” *Offshore wind Energy*, EWEA Special Topic Conference, Brussels, Belgium, 2001.

[9] Hasager, C.B., Furevik, B., Dellwik, E., Sandven, S. Frank, H.P., Jensen, N.O., Astrup, P., Joergensen, B.H., Rathmann, O., Barthelmie, R.; Johannessen, O., Gaudiosi, G.; Christensen, L.C., 2001 Satellite images used in offshore wind resource assessment. 2001 *Proceedings of the European Wind Energy Conference and exhibition* (EWEC), Copenhagen (DK), 2-6 July 2001, pp. 673-677.

[10] Y. Quilfen, B. Chapron, T. Elfouhaily, K. Katsaros, & J. Tournadre, Observation of tropical cyclones by high-resolution scatterometry. J. Geophys. Research, **103, C4**, (1998) 7767-7786

[11] A. Stoffelen, D.L.T. Anderson, Wind retrieval and ERS-1 scatterometer radar backscatter measurements. Advance Space Research, **13**, (1993) 53-60

[12] DWD (1999-2000) European Meteorological Bulletin surface charts from DWD in resolutions 1:30.000.000 and 1:60.000.000. Deutsher Wetterdienst, Offenbach, Germany.

[13] Pryor, S., Barthelmie, R., Hasager, C.B. 2002. Can satellite sampling of offshore wind represent wind speed distributions? Proceedings of Global Windpower Conference, Paris, 2-5 April, 2002 (this issue).